Cholesterol esterification by ACAT2 is essential for efficient intestinal cholesterol absorption: evidence from thoracic lymph duct cannulation[S]

Tam M. Nguyen,[1] Janet K. Sawyer, Kathryn L. Kelley, Matthew A. Davis, and Lawrence L. Rudel[2]

Department of Pathology, Wake Forest University School of Medicine, Winston-Salem, NC

Abstract The hypothesis tested in this study was that cholesterol esterification by ACAT2 would increase cholesterol absorption efficiency by providing cholesteryl ester (CE) for incorporation into chylomicrons. The assumption was that absorption would be proportional to *Acat2* gene dosage. Male ACAT2$^{+/+}$, ACAT2$^{+/-}$, and ACAT2$^{-/-}$ mice were fed a diet containing 20% of energy as palm oil with 0.2% (w/w) cholesterol. Cholesterol absorption efficiency was measured by fecal dual-isotope and thoracic lymph duct cannulation (TLDC) methods using [^{3}H]sitosterol and [^{14}C]cholesterol tracers. Excellent agreement among individual mice was found for cholesterol absorption measured by both techniques. Cholesterol absorption efficiency in ACAT2$^{-/-}$ mice was 16% compared with 46–47% in ACAT2$^{+/+}$ and ACAT2$^{+/-}$ mice. Chylomicrons from ACAT2$^{+/+}$ and ACAT2$^{+/-}$ mice carried ~80% of total sterol mass as CE, whereas ACAT2$^{-/-}$ chylomicrons carried >90% of sterol mass in the unesterified form. The total percentage of chylomicron mass as CE was reduced from 12% in the presence of ACAT2 to ~1% in ACAT2$^{-/-}$ mice. Altogether, the data demonstrate that ACAT2 increases cholesterol absorption efficiency by providing CE for chylomicron transport, but one copy of the *Acat2* gene, providing ~50% of ACAT2 mRNA and enzyme activity, was as effective as two copies in promoting cholesterol absorption.—Nguyen, T. M., J. K. Sawyer, K. L. Kelley, M. A. Davis, and L. L. Rudel. **Cholesterol esterification by ACAT2 is essential for efficient intestinal cholesterol absorption: evidence from thoracic lymph duct cannulation. *J. Lipid Res.* 2012.** 53: **95–104.**

Supplementary key words chylomicron • lipoprotein metabolism • cholesterol transport

Elevated plasma cholesterol concentration is widely accepted as a risk factor for accelerated atherosclerosis and coronary heart disease (CHD) (1, 2). Because there are positive correlations among cholesterol absorption, plasma cholesterol concentrations, and CHD risk, understanding the physiology of intestinal sterol transport can provide new therapeutic strategies for preventing cardiovascular disease (CVD) (3–6). Whole-body cholesterol homeostasis is achieved by the balance among de novo synthesis, intestinal excretion, and absorption from diet (7). While the molecular mechanisms of cholesterol synthesis are well described, our understanding of the mechanisms governing cholesterol absorption and excretion still remains incomplete.

Early studies in humans as well as various animal species, including monkeys, dogs, rabbits, and rats, have documented that 70–80% of newly absorbed cholesterol is transported in the form of cholesteryl ester (CE) (8–13). Detailed characterizations of the enzyme acyl CoA: cholesterol acyl transferase (ACAT) have revealed two different isoforms, designated as ACAT1 and ACAT2 (14, 15), with different tissue distributions and apparently distinct functions (16). In African green monkeys, ACAT1 is ubiquitously expressed in many tissues, whereas ACAT2 is exclusively expressed in the liver and small intestine (17), a finding similar to what is seen in mice (15). Relevant to humans is the observation that dietary cholesterol or saturated fat feeding leads to the accumulation of larger, more CE-rich LDL particles in man (18), which has also been documented in nonhuman primates (19, 20). In the enterocyte, ACAT2 has long been suggested to play

This work was funded by National Institutes of Health Grant HL-49373 and by the Howard Hughes Medical Institute Gilliam Fellowship for Advanced Studies. Its contents are solely the responsibility of the authors and do not necessarily represent the official views of the National Institutes of Health or other granting agencies.

Manuscript received 18 July 2011 and in revised form 11 October 2011.

Published, JLR Papers in Press, November 1, 2011
DOI 10.1194/jlr.M018820

Abbreviations: ABCG5, ATP-binding cassette transporter 5; AU, arbitrary unit; CE, cholesterol ester; CHD, coronary heart disease; CVD, cardiovascular disease; FC, free cholesterol; FDI, fecal dual-isotope; GI, gastrointestinal; HDL-C, high density lipoprotein cholesterol; LDL-C, low density lipoprotein cholesterol; PL, phospholipid; SI, small intestine; TCA, trichloroacetic acid; TG, triglyceride; TLDC, thoracic lymph duct cannulation; TPC, total plasma cholesterol; VLDL-C, very low density lipoprotein cholesterol.

[1] Present address of T. M. Nguyen: Department of Pathology and Laboratory Medicine, University of North Carolina at Chapel Hill, Chapel Hill, NC 27599-7525.

[2] To whom correspondence should be addressed.
e-mail: lrudel@wfubmc.edu

[S] The online version of this article (available at http://www.jlr.org) contains supplementary data in the form of two figures and one table.

a critical role in cholesterol absorption by catalyzing the esterification reaction converting free cholesterol (FC) into CE, which can then be assembled into the core of chylomicron particles (21, 22). However, no study to date has directly demonstrated that cholesterol esterification by ACAT2 plays a crucial role in chylomicron cholesterol transport.

The objective of this study is to directly investigate the mechanistic role of ACAT2 in regulating intestinal cholesterol absorption efficiency and cholesterol transport by chylomicrons. We hypothesized that, by catalyzing CE formation in the enterocyte, ACAT2 increases cholesterol absorption proportionally to *Acat2* gene dosage. The role of ACAT2 in intestinal sterol absorption is of special interest because the physicochemical state of the cholesterol molecule determines its fate in the body. FC is soluble in membrane phospholipids and represents an important structural component of cellular membranes, such as the plasma membrane and endoplasmic reticulum (ER) membrane. FC is also a component of the surface phospholipid monolayer of a lipoprotein, where it can undergo diffusional exchange in chyle and in blood (23). By contrast, CE is mostly insoluble in membranes and must be packaged into lipid droplets or incorporated into the core of lipoprotein particles for export out of the cell. We hypothesized that interruptions in intestinal CE formation in $ACAT2^{+/-}$ or $ACAT2^{-/-}$ mice will be associated with decreased cholesterol absorption efficiency, and we suspected that as the copy number of ACAT2 allele decreased, a stair-step decrease in cholesterol absorption efficiency would occur.

To directly document metabolic aspects of cholesterol absorption, a surgical technique of thoracic lymph duct cannulation (TLDC) was used in mice to directly investigate the physiological mechanisms of how newly absorbed cholesterol is transported and delivered into the circulation via intestine-derived lipoproteins, primarily chylomicrons. As documented by Gage and Fish in 1924 (24), chylomicron particles in thoracic duct lymph of humans and various animal models are the primary carriers of dietary lipids. Fat-soluble dyes were used to show that all lymph from the gastrointestinal (GI) tract and the lower extremities of the body pools into the cisterna chyli, then flows along the aorta up the thoracic duct and joins the venous system at the subclavian vein. Now almost ninety years later, we have been able to quantitatively collect thoracic duct lymph during active lipid absorption in genetically engineered mice to better define the physiological mechanisms of a specific protein of interest–ACAT2–in intestinal cholesterol absorption and transport. The ACAT2-deficient mouse model used in this study was originally described by Buhman et al. (25), who found that $ACAT2^{-/-}$ mice possessed complete resistance to diet-induced hypercholesterolemia and cholesterol gallstone formation, whereas $ACAT2^{+/+}$ and $ACAT2^{+/-}$ mice developed severe and intermediate levels of gallstones, respectively. These findings suggest that there may be a gene-dosage effect of *Acat2* on cholesterol absorption and metabolism.

MATERIALS AND METHODS

Animals and diets

All mice used in these studies were housed in a clean barrier facility within the Animal Resources Program (AALAC accredited) at Wake Forest School of Medicine (WFSM), and the WFSM Institutional Animal Care and Use Committee approved all protocols prior to execution. Male $ACAT2^{+/+}$, $ACAT2^{+/-}$, and $ACAT2^{-/-}$ mice were colony bred on a pure C57Bl/6 background and maintained on rodent chow before entering the studies at 10–15 weeks of age. During both studies, mice were fed a semisynthetic saturated fat diet containing 20% of energy as palm oil and 0.2% cholesterol (w/w) (26) for five weeks. In the first study, a baseline blood sample was taken from mice (n = 8–13/genotype) prior to study initiation, and an additional blood sample was taken after two weeks of saturated fat diet feeding. Then, a three-day fecal collection was performed for indirect measurement of cholesterol absorption by fecal dual-isotope (FDI) method at week 3. At week 5, animals (n = 7–9/genotype) underwent TLDC surgery for direct assessment of sterol absorption, followed by euthanasia. In a second age-matched study, mice (n = 5/genotype) were fed the saturated fat diet for 5 weeks, followed by euthanasia for tissue collection.

Plasma lipid concentrations

Plasma cholesterol concentrations were analyzed at baseline (rodent chow) and after two weeks of saturated fat diet feeding. Prior to blood sampling, mice were fasted for 4 h. Blood was obtained from the superficial submandibular vein, and plasma was collected after centrifugation of blood at 1700 *g* for 15 min at 4°C. Total plasma cholesterol (TPC) and plasma triglyceride (TG) concentrations were analyzed using the Cholesterol/HP (Roche Diagnostics) and Triglyceride (Wako Chemicals) enzymatic kits, respectively, according to the manufacturers' instructions. Percentage plasma cholesterol distribution among lipoprotein classes was determined after separation by gel filtration chromatography by a method similar to that described previously (27). By multiplying the percentages of lipoprotein cholesterol distribution by the TPC concentration, cholesterol concentrations were determined for VLDL, LDL, and HDL.

Liver and intestine collection

After a 4 h fast, mice (n = 5/genotype) were anesthetized by intramuscular injection with 2 μg/g body weight of 50 mg/ml ketamine:10 mg/ml xylazine solution. Exsanguination was achieved by cardiac puncture, and the circulatory system was flushed with 0.9% NaCl. Livers were removed, minced, and snap-frozen in liquid nitrogen. The small intestine was cut into 5 equal-length segments, flushed clean with 0.9% NaCl, and snap-frozen in liquid nitrogen. All tissues were stored at −80°C until processing.

Microsomal ACAT2 enzymatic activity assay

Frozen liver and small intestine segments were crushed using a mortar and pestle chilled in liquid nitrogen to prevent tissue thawing. Approximately 200–300 mg of frozen crushed tissue was homogenized in ACAT homogenization buffer (0.25 M sucrose, 1 mM EDTA, 0.1 M K_2HPO_4, pH 7.4) in the presence of protease inhibitor cocktail (20 μl for SI, 10 μl for liver, Sigma). Microsomes were isolated and ACAT assays were performed by a similar method to that described previously (28). Relative ACAT enzyme activity was expressed as nanomole CE synthesized per milligram microsomal protein per minute (nmol/mg/min). Duplicate assays were performed for each tissue pool (n = 5/genotype) in the absence and presence of 0.1 mM pyripyropene A (PPPA), an

ACAT2-specific inhibitor. For each tissue pool, ACAT2 activity was calculated by subtracting values of PPPA-treated samples from values of untreated samples; ACAT1 activity was determined as the difference between total ACAT and ACAT2 activities.

Real-time PCR analysis of mRNA expression

Total RNA was extracted from 50–100 mg of crushed frozen small intestine segments and liver tissue with Trizol reagent (Invitrogen) using the manufacturer's instructions. With the exceptions of *Acat2, Npc1l1*, and *Abcg5* genes that were analyzed as individual samples (n = 5/genotype), assays for other lipid metabolism genes in supplementary Table I were performed with equal amounts of cDNA pooled from five mice of each genotype. Real-time polymerase chain reaction (RT-PCR) was used to analyze two pools per tissue for each genotype as described previously (29). Ct values were calculated based on fluorescence measurements and entered into an equation (arbitrary unit = $1 \times 10^9 \times e^{(0.6931 \times Ct)}$) to determine arbitrary units (AU). All results were normalized by mRNA expression of cyclophilin, a housekeeping gene, within the same tissue sample or sample pool.

Cholesterol absorption analysis by fecal dual-isotope method

Because the fecal dual-isotope (FDI) method is well accepted in the literature as an indirect method for estimating cholesterol absorption efficiency (30), it was used to validate the direct evaluation of cholesterol absorption by TLDC. After two weeks of saturated fat diet feeding, mice (n = 7–9/genotype) were gavaged with 25 μl soybean oil mixture containing 0.034 μCi 4-[^{14}C]cholesterol (American Radiolabeled Chemicals) and as a nonabsorbable marker, 0.088 μCi 22,23-[^{3}H]sitosterol (New England Nuclear). A very low dose of radioactive sterols was used to avoid confounding readings in the subsequent TLDC experiments performed two weeks later. Feces were collected for three days while the mice were individually maintained in wire-bottomed cages with free access to food and water. Dried fecal pellets were crushed into a fine powder and approximately 300 mg of fecal powder along with 5α-cholestane (internal standard) were saponifed and extracted with hexane as described (29). To estimate percent cholesterol absorption, the radioactivity in the total lipid extract was quantified in a liquid scintillation spectrometer (Beckman Coulter LS 6500) and the disintegrations per minute (dpm) were entered into the following equation: [(^{14}C/^{3}H dose − ^{14}C/^{3}H feces) / ^{14}C/^{3}H dose] × 100 = % cholesterol absorption efficiency.

Cholesterol absorption analysis by thoracic lymph duct cannulation

Subsequent to fecal collection for FDI measurements, mice were returned to regular cages and saturated fat diet feeding continued for an additional two weeks. A modified version of the thoracic lymph duct cannulation (TLDC) procedure previously described by Ionac (31) was used. Thirty minutes prior to surgery, mice were gavaged with 25 μl soybean oil to facilitate visualization of the lymphatic vessels and were injected subcutaneously with ketoprofen (5 mg/kg body weight). Ketoprofen, a nonsteroidal anti-inflammatory drug, was used for analgesia to avoid the possibility of opioid-induced postoperative ileus and drowsiness.

The thoracic lymph duct cannula consisted of two tubes: a 5 cm long RenaSil Silicone tubing (0.939 mm OD × 0.635 mm ID, Braintree Scientific) connected to a 10 cm long silicone tubing (1.651 mm OD × 0.762 mm ID, HelixMark). Prior to surgery, mice were anesthetized with isoflurane (4% for induction, 2–3% for maintenance) positioned on their right side on a 37°C heating pad, and monitored for maintenance of body temperature (Microtherma 2, Braintree Scientific). A left subcostal incision was made to visualize the abdominal cavity. Then to cannulate the proximal duodenum, a small incision was made through the wall of the antrum of the stomach, and a 60 cm RenaSil Silicone tubing (0.939 mm OD × 0.635 mm ID, Braintree Scientific) was inserted into the stomach, through the pyloric sphincter and into the proximal duodenum (∼5mm). After the duodenal cannula was fastened into place using silk suture (4-0), a mixed micelle solution was constantly infused into the duodenum via the cannula at a rate of 300 μl/hr using a syringe pump (Harvard Apparatus) for the remainder of the 8 h study. The micelle solution contained 3 mM egg lecithin, 16 mM oleic acid, and 54 mM NaTC in a complete PBS (6.75 mM Na_2HPO_4, 16.5 mM NaH_2PO_4, 115 mM NaCl, 15 mM KCl, 10 mM Glc, 1 mM $CaCl_2$, pH 6.4) (Sigma). After cannulating the duodenum, a bolus dose of radioactive micelle solution (4.4 μCi 22,23-[^{3}H]sitosterol and 2.2 μCi 4-[^{14}C]cholesterol as tracers, 3.8 mM cold cholesterol, 0.7 mM cold sitosterol, 35.2 mM egg lecithin, 200 mM NaTC in 120 μl PBS, pH 7.5) was injected directly into the duodenum just below the pyloric sphincter, and the injection site was glued with Hexabond tissue adhesive to ensure that no leakage occurred.

Abdominal organs were carefully retracted and connective tissue was dissected away to visualize the milky-colored cisterna chyli and the TLD. The TLD cannula, which was preloaded with 50 IU heparin/ml saline, was gently inserted into the TLD vessel, and Hexabond tissue adhesive was used to glue the surrounding tissue to the cannula to tightly secure the tubing in place. The cannulation was considered successful if cloudy lymph flowed into the cannula and heparinized saline flowed to the external end of the tubing. Upon successful cannulation, organs were returned to their correct anatomical locations, the abdominal muscle wall was closed with a running suture, the skin was glued together with adhesive, and the abdomen was stabilized with several layers of wound tape. The mouse was restrained on an exercise wheel to allow for free body movement. Lymph was drained via the cannula into an Eppendorf tube, containing 5 μl protease inhibitor cocktail (Sigma) plus 5% EDTA and 5% sodium azide, for 8 h with tubes changed hourly.

Percentage sterol absorption was quantitatively measured in each animal by quantifying the dpm of [^{14}C]cholesterol and [^{3}H]sitosterol in whole lymph from each hourly collection and dividing the values by the total dpm in the bolus dose injected into the duodenum. Cholesterol absorption was directly quantified by sampling lymph produced during active lipid absorption, and the cumulative percentage of the radioactive dose in thoracic duct lymph by the end of 8 h was calculated as the cholesterol absorption efficiency of each individual animal. Experiments were stopped after 8 h, because trial experiments of up to 12 h of lymph collection did not yield more appreciable amounts of radioactivity in the lymph.

Chylomicron isolation and particle composition analyses

Lymph was collected at room temperature and stored at 4°C until processed. Chylomicron particles were isolated by ultracentrifugation of whole lymph under a layer of saline (0.9% NaCl, 0.05% EDTA, 0.05% Na azide) at 43,600 *g* for 4 h at 15°C in a 2 ml Quick-Seal polyallomer tube (Beckman Coulter). The packed layer of chylomicrons at the top was separated from the bottom fraction by cutting the tube with a Beckman tube slicer. Chylomicrons were resuspended gently in a total volume of 1 ml with the same saline solution. Aliquots of isolated chylomicrons (n = 5/genotype) were used to determine particle composition. Chylomicron protein concentrations were quantified using a modified Lowry assay (32). Because the chylomicron solution was very cloudy, absorbance could not be measured accurately, so chloroform was added with vortexing to extract lipids. The tubes were

then centrifuged at 1,871 *g* for 30 min at room temperature, and the absorbance of the clarified blue colored top phase was measured at 595 nm wavelength in a spectrophotometer.

Chylomicron lipids were extracted using the Bligh-Dyer method (33). Phospholipid mass was measured by a colorimetric inorganic phosphorous assay (34). For chylomicron TG mass, the total lipid extract was dissolved in 1% Triton-$CHCl_3$, the solvent was evaporated, the dissolved lipids were resuspended in deionized water, and the TG concentration was measured by an enzymatic kit (Wako) according to the manufacturer's instructions. Chylomicron sterol composition was analyzed by GC with a similar method to that described previously (26). The differences between total cholesterol (TC) mass and FC mass were multiplied by 1.67 to calculate CE mass. The percentages of radioactivity in free sterols and sterol esters were quantified by a liquid scintillation spectrometer after lipid class separation by thin-layer chromatography. Because the FC/TC values did not vary from hour to hour during the entire experiment, we averaged values from all 8 time points for each mouse and reported the overall average of 5 mice per genotype group. Chylomicron size was measured by dynamic light-scattering using the Zetasizer Nano (Malvern Instruments), following manufacturer's instructions. Chylomicron particles from lymph collections at hour 3 and hour 4 were measured, as these fractions made up the peak of the percentage cholesterol absorption curve during the 8 h time course. Each sample was measured in duplicate to derive the average chylomicron diameter for each animal (n = 5/genotype).

Chylomicron apolipoprotein profile

To quantify the relative abundance of each apolipoprotein class, trichloroacetic acid (TCA) precipitation of chylomicron proteins from the hour 3 lymph collection (n = 3/genotype) was used, then apolipoproteins were separated on 4–20% Tris-Glycine SDS-PAGE gels (Lonza). The gels were stained with Coomassie blue as previously described (35). Quantification of the apolipoprotein bands was performed using the Alpha-Innotech Gel Imager according to manufacturer's instructions.

Statistical analyses

Using GraphPad Prism statistical software v4 (GraphPad Software Inc.), we analyzed data by one-way ANOVA with Tukey posthoc tests or two-way ANOVA with Bonferroni posthoc tests. Differences were considered statistically significant at $P < 0.05$ and are indicated by different superscript letters.

RESULTS

Total plasma cholesterol (TPC) and plasma TG concentrations were measured in $ACAT2^{+/+}$, $ACAT2^{+/-}$, $ACAT2^{-/-}$ mice at baseline (chow diet) and after two weeks of saturated fat diet feeding to determine whether *Acat2* gene dosage altered plasma lipid concentrations in a gene dose-dependent manner (**Fig. 1**). All mice entered the study with similar TPC of ~100 mg/dl on a chow diet. However, after two weeks on the saturated fat diet, both the $ACAT2^{+/+}$ and $ACAT2^{+/-}$ mice exhibited a ~100% increase in TPC, whereas $ACAT2^{-/-}$ mice had only a ~30% increase (Fig. 1A). VLDL-c concentration did not change significantly (data not shown). Most of the increase occurred in concentrations of LDL-c (Fig. 1B) and HDL-c (Fig. 1C). On the other hand, plasma TG concentration (Fig. 1D) decreased on the saturated fat diet among all genotypes, but it was generally higher in $ACAT2^{-/-}$ mice than in mice

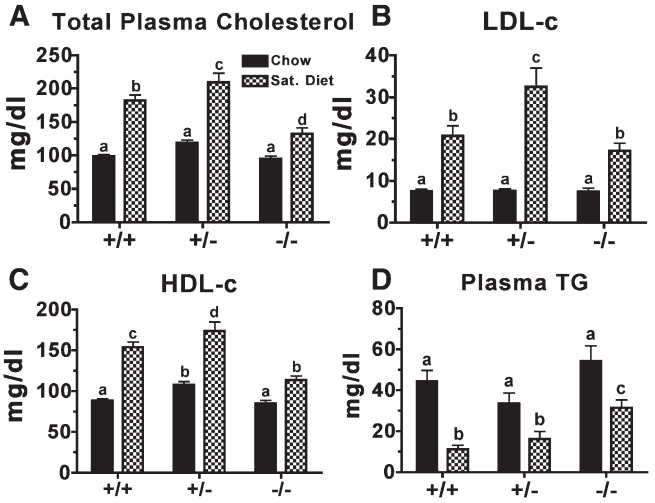

Fig. 1. Diet effects on plasma cholesterol and triglyceride concentrations in male $ACAT2^{+/+}$, $ACAT2^{+/-}$, and $ACAT2^{-/-}$ mice. Plasma was collected after centrifugation of blood from mice fed rodent chow and two weeks of saturated fat diet (20% of energy as palm oil and 0.2% (w/w) cholesterol). (A) Total plasma cholesterol concentrations measured using the cholesterol/HP enzymatic reagents from Roche Diagnostics. (B) LDL cholesterol and (C) HDL cholesterol concentrations determined by gel filtration chromatography. (D) Triglyceride concentrations measured using reagents from Wako Chemicals. Data represent mean ± SEM (n = 8–13/genotypes). Data were analyzed by two-way ANOVA with Bonferroni posthoc tests. Different letters designate statistically significant differences ($P < 0.05$).

with functional ACAT2, a well-documented phenotype observed in ACAT2-deficient mice (36–38). Overall, $ACAT2^{-/-}$ mice displayed a blunted diet-induced elevation in plasma cholesterol concentration relative to that observed in $ACAT2^{+/+}$ and $ACAT2^{+/-}$ mice.

Microsomal ACAT assays were used to measure relative expression of ACAT2 enzyme activity in each section of small intestine (SI) and compared with that of the liver (**Fig. 2A**). The data show that higher levels of ACAT2 enzyme activity existed in the proximal portion of the intestine and that this activity was relatively higher in these segments of the SI than in the liver. Relative to ACAT2, ACAT1 enzyme activity was less than one tenth that of ACAT2 activity in both the SI and in the liver (data not shown). Moreover, ACAT1 activity was similar in $ACAT2^{-/-}$ mice as in $ACAT2^{+/+}$ and $ACAT2^{+/-}$ mice. $ACAT2^{+/-}$ mice had ~50% less ACAT2 activity than $ACAT2^{+/+}$ mice in all segments of the SI and in the liver, whereas no activity was detected in any sample from $ACAT2^{-/-}$ mice.

ACAT2 mRNA expression also exhibited the same gene dose-dependent reduction as ACAT2 activity (Fig. 2B). *Acat2* gene expression was ~50% less in $ACAT2^{+/-}$ than $ACAT2^{+/+}$ mice, and it was undetectable in $ACAT2^{-/-}$ mice. Interestingly, the pattern of ACAT2 mRNA abundance down the length of the small intestine was different from the pattern of enzyme activity, with SI segments 3–5 having apparently higher levels of mRNA than enzyme activity.

Gene expression was also measured for *Npc1l1* and *Abcg5*. *Npc1l1* mRNA expression (Fig. 2C) was highest in

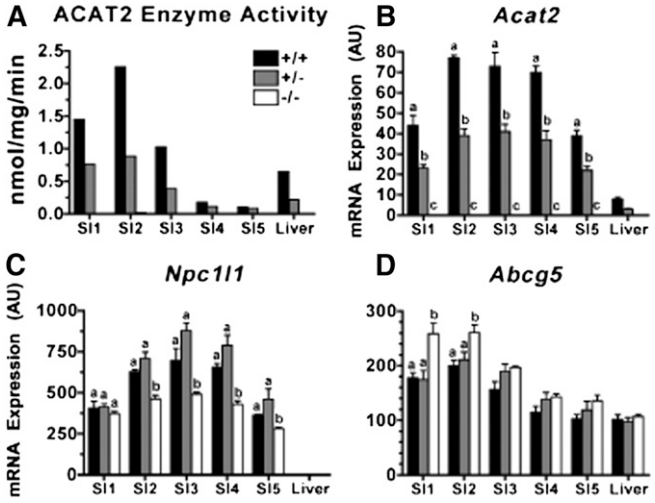

Fig. 2. Impact of *Acat2* gene dosage on ACAT2 enzyme activity and *Acat2*, *Npc1l1*, and *Abcg5* mRNA expression in five segments of small intestine (SI) compared with liver. (A) Microsomal ACAT2 activity of tissue pools (n = 5/genotype). (B) *Acat2*, (C) *Npc1l1*, and (D) *Abcg5* mRNA expression from individual samples are expressed as mean ± SEM (n = 5/genotype). All values for mRNA expressions are arbitrary units (AU) derived from real-time-PCR data normalized to mRNA expression of cyclophilin, a housekeeping gene, within the same sample. Different letters designate statistically significant differences ($P < 0.05$) within the same tissue, as measured by two-way ANOVA and Bonferroni posthoc tests.

segments 2–4, not unlike *Acat2*. *Npc1l1* expression was significantly lower in all SI segments of ACAT2$^{-/-}$ mice compared with those with functional ACAT2, although the gene dosage effect was not apparent as no differences were observed between ACAT2$^{+/+}$ and ACAT2$^{+/-}$ mice. The pattern of *Abcg5* expression in SI segments was also similar to that of *Acat2* and *Npc1l1*, being higher in proximal segments of the small intestine. However, *Abcg5* expression was significantly higher in the proximal segments of the SI in ACAT2$^{-/-}$ mice. These data were in general agreement with previously published data (39).

Fig. 3 shows data on the percentage of intestinal cholesterol absorption measured by two methods: FDI and TLDC. Both methods yielded comparable values for cholesterol absorption efficiency across all three genotypes of mice. The average (± SEM) cholesterol absorption percentages in ACAT2$^{+/+}$ (42.9 ± 8.25% for FDI versus 46.08 ± 5.73% for TLDC) and ACAT2$^{+/-}$ (42.01 ± 5.10% for FDI versus 47.12 ± 4.51% for TLDC) mice were similar between methods; however, ACAT2$^{-/-}$ mice had significantly lower percentages of cholesterol absorption (12.00 ± 2.61% for FDI versus 15.61 ± 2.64% for TLDC). Values among individual animals for each method are presented in Fig. 3B to show that both methods of estimating cholesterol absorption were, in general, comparable among individual mice.

Fig. 4 shows the cumulative percentages of [^{14}C]cholesterol and [^{3}H]sitosterol dose recovered in thoracic duct lymph of all three genotypes after TLDC. A distinct effect of the ACAT2 genotype was apparent in [^{14}C]cholesterol accumulation in lymph. From hours 2–8 of lymph collection, significantly less [^{14}C]cholesterol appeared in lymph of the ACAT2$^{-/-}$ mice compared with ACAT2$^{+/+}$ and

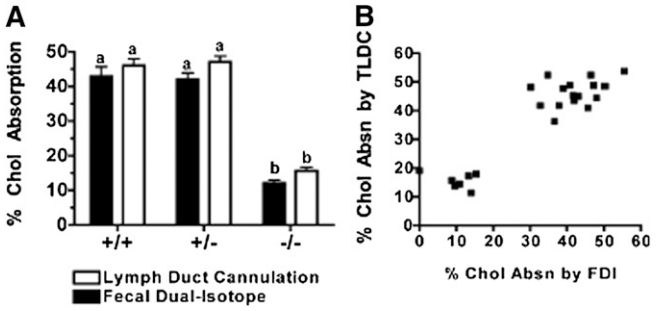

Fig. 3. Measurement of cholesterol absorption efficiency by FDI and TLDC. (A) Estimation of percentage cholesterol absorption by FDI method was derived from extraction of crushed feces collected for three days; direct measurement of percentage cholesterol absorption by TLDC was reported as the percentage of total [^{14}C] cholesterol dose recovered in lymph after 8 h collection. See Materials and Methods for details. Data are expressed as mean ± SEM (n = 7–9/genotype). Different letters designate statistically significant differences ($P < 0.05$) as measured by two-way ANOVA and Bonferroni posthoc tests. (B) Percent cholesterol absorption values derived from FDI and TLDC methods for 24 individual animals.

ACAT2$^{+/-}$ mice. The fact that this difference was seen throughout the experiment demonstrates that this trend represents the physiologic behavior of newly absorbed cholesterol. Moreover, no difference was seen between the ACAT2$^{+/+}$ and ACAT2$^{+/-}$ mice, indicating that decreasing ACAT2 availability by 50% did not change the efficiency of cholesterol absorption. Very little [^{3}H]sitosterol absorption (only 2–3% of the dose) accumulated in lymph over the 8 h experiment, and no effect of ACAT2 gene dosage was seen.

All experiments were conducted over an 8 h time course, because the percentages of [^{14}C]cholesterol recovered in lymph per hourly collection peaked between hours 2 and 4, and then dramatically decreased to only 3.87 ± 1.08%, 3.47 ± 0.29%, and 1.99 ± 0.74% in ACAT2$^{+/+}$, ACAT2$^{+/-}$, and ACAT2$^{-/-}$ mice, respectively, at the end of 8 h

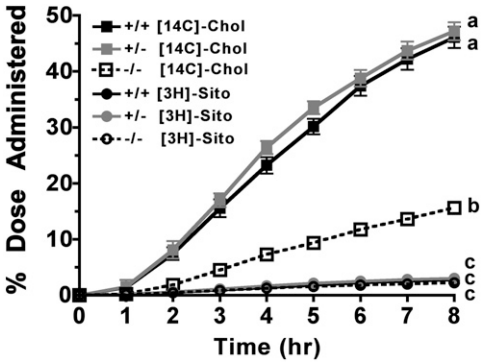

Fig. 4. Cumulative radioactive sterol appearance in thoracic duct lymph. Using a dual-channel isotope scintillation spectrometer, [^{14}C]cholesterol and [^{3}H]sitosterol disintegrations per minute were measured in aliquots of whole lymph from hourly collections. Data are expressed as percentage of accumulated radioactive sterol dose recovered in collected lymph for each animal and represent mean ± SEM (n = 7–9/genotype). Different letters denote statistically significant differences ($P < 0.05$) at 8 h as measured by two-way ANOVA and Bonferroni posthoc tests.

(supplementary Fig. I-A). The percentage of [^{3}H]sitosterol absorption decreased to ~0.2% in all genotypes of mice (supplementary Fig. I-B). The experiments were terminated after 8 h because longer lymph collections of up to 12 h in some trial animals did not yield more appreciable amounts of radioactivity recovery in lymph (data not shown). Chylomicron TG mass appeared to be fairly constant in all genotypes throughout the experiment (supplementary Fig. I-C). No statistically significant differences were found among all genotypes at the hour 8 time point.

At the end of lymph collection, less than 1% of the total radioactive dose administered was found in the plasma and liver of these animals (data not shown), strongly indicating that the cannula had remained in place throughout the experiment and that it provided a quantitative collection of newly absorbed cholesterol. This finding also suggests that intestine-derived HDL particles did not contribute significantly to cholesterol absorption as has been suggested by other researchers (29, 40, 41).

Performing TLDC provided an opportunity in which the enterocyte, as the only cell between the gut lumen and the lymph collection, was effectively isolated to study the characteristics of chylomicrons that are transporting newly absorbed cholesterol. With this method, we directly sampled what the enterocyte secreted into lymph during active absorption of lipids from the gut lumen. To further evaluate ACAT2 enzyme function, the average (± SEM) percentage distribution of chylomicron radioactivity into free sterols versus sterol esters was examined (**Fig. 5**). We found 85.5 ± 1.3% and 80.5 ± 1.4% of [^{14}C]cholesterol in ACAT2$^{+/+}$ and ACAT2$^{+/-}$ chylomicrons, respectively, in the ester form, whereas ACAT2$^{-/-}$ chylomicrons carried 84.0 ± 4.1% in the unesterified form (Fig. 5A). The enzymatic source of any sterol ester in the remaining ~15% that could have been formed by the intestine of ACAT2$^{-/-}$ mice is unknown. It could have come from ACAT1, but this seems unlikely as ACAT1 has not been found in the enterocyte (16). Or, it could have come from some the wax esterases described by Turkish et al. (42). We could not identify the fatty acid species associated with this fraction. The percentage of [^{3}H]sitosterol esterified was much lower at 20.7 ± 1.3% and 17.6 ± 2.5% in ACAT2$^{+/+}$ and ACAT2$^{+/-}$ chylomicrons, respectively, whereas esterified sitoserol was almost undetectable in ACAT2$^{-/-}$ chylomicrons (Fig. 5B). These data strongly support the concept that ACAT2 preferentially esterifies cholesterol over phytosterols, as previously suggested (43).

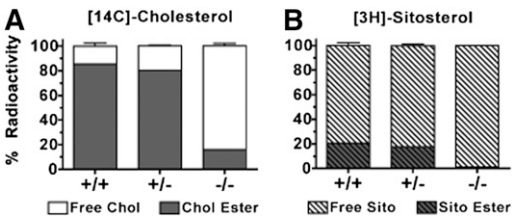

Fig. 5. Relative percentage of radioactivity in chylomicron free sterols and sterol esters. Total lipid extracts of isolated chylomicrons were separated by thin-layer chromatography into free sterols and sterol esters. (A) Relative percentage of [^{14}C]cholesterol in free sterol and sterol esters. (B) Relative percentage of [^{3}H]sitosterol in free sterol and sterol esters. Data represent mean ± SEM (n = 5/genotype).

No differences were observed in the appearance rates of chylomicron protein, FC, or TG mass (**Fig. 6A**, C, D, respectively) across all three genotypes. Although phospholipid (PL) mass secretion appeared to be slightly lower in ACAT2$^{-/-}$ mice than in their counterparts (Fig. 6B), PL made up about 11% of the total particle mass in chylomicrons isolated from all three genotypes (**Table 1**). The striking difference was that ACAT2$^{-/-}$ mice secreted 18-fold less CE into chylomicrons than did ACAT2$^{+/+}$ and ACAT2$^{+/-}$ mice, which secreted CE at similar rates (Fig. 6E). This finding provides novel and persuasive evidence demonstrating that intestine-derived CE in chylomicrons originates from ACAT2-specific cholesterol esterification.

Chylomicron particle size (averaged ~150 nm) (**Fig. 7**) and chylomicron surface:core ratios (Table 1) were similar across all three groups, even though particle core composition was significantly altered in the absence of ACAT2. The percentage of chylomicron particle mass as CE was reduced from 12.3 ± 1.9% and 11.1 ± 2.9% in ACAT2$^{+/+}$ and ACAT2$^{+/-}$, respectively, to only 1.0 ± 0.4% in ACAT2$^{-/-}$ chylomicrons; this reduction was compensated for by an increase in TG as the percentage of total mass.

In addition to particle mass composition, apolipoprotein profiles and the relative percentage composition of each apolipoprotein were examined in each mouse genotype (**Fig. 8**, **Table 2**). There was variability, but no statistically significant differences were found in apolipoprotein profiles among individual animals. Statistically significant differences in the average percentage composition of apolipoproteins from individual animals throughout the 8 h time course were not found (data not shown). Interestingly, the apolipoprotein patterns in mouse chylomicrons appeared similar to those isolated from nonhuman primates (21) and rats (13), with the following order of abundance: ApoC > ApoA-IV > ApoA-I > ApoB.

DISCUSSION

This study provides new evidence demonstrating a specific role for ACAT2 in intestinal cholesterol absorption and transport in chylomicrons. The use of thoracic duct lymph collection during absorption of a meal shows that, in mice, more efficient cholesterol absorption requires CE incorporation into chylomicrons, whereas the movement of newly absorbed cholesterol through the enterocyte into HDL particles is minimal. As evidenced from administering a single bolus of radiolabeled cholesterol during absorption of a meal, the role of ACAT2 extends across the entire time course of cholesterol absorption. Radioactive tracer data and chylomicron sterol mass analyses agree that CE formation utilizes chylomicron particles for cholesterol transport out of the enterocyte into lymph and that the lack of cholesterol esterification by ACAT2 is associated with inefficient cholesterol absorption. Collectively, our results demonstrate that, in

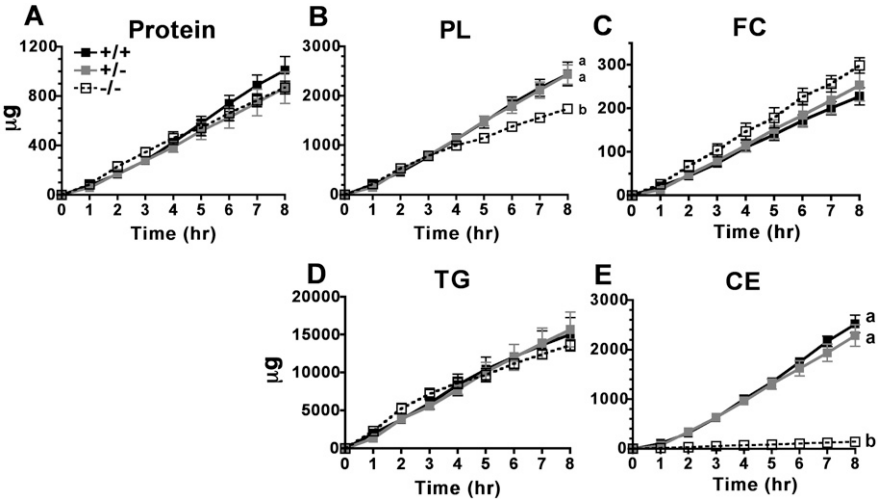

Fig. 6. Cumulative chylomicron particle mass appearance over 8 h. Isolated chylomicrons were assayed for micrograms of (A) protein, (B) phospholipids, (C) free cholesterol, (D) triglyceride, and (E) cholesteryl ester per hourly collection of lymph. Data are expressed as mean ± SEM (n = 5/genotype). Different letters denote statistically significant differences ($P < 0.05$) as measured by two-way ANOVA and Bonferroni posthoc tests.

the enterocyte, ACAT2 is the major enzyme for cholesterol esterification. Further, we had hypothesized that if cholesterol esterification by ACAT2 increased cholesterol absorption efficiency, the extent of absorption would be proportional to *Acat2* gene dosage. However, this was not found, as the ACAT2$^{+/-}$ mice exhibited the same absorption efficiency as the ACAT2$^{+/+}$ mice. Intestinal ACAT2 is apparently present in excess in wild-type C57Bl/6 mice, and half the amount of ACAT2 in the small intestine is apparently sufficient to provide for efficient cholesterol esterification and absorption.

Based on our mRNA data, the absence of *Acat2* in the intestine appeared to be associated with a downregulation *of Npc1l1* expression, a finding in agreement with previously published data (29, 39, 41, 44). This decrease occurred in all segments of the SI (Fig. 2C). Lower NPC1L1 could have contributed to the decrease in cholesterol absorption efficiency in ACAT2$^{-/-}$ mice by limiting the uptake of cholesterol into the enterocyte, but it is not clear whether the decrease in *Npc1l1* expression would be a primary versus a secondary contributor to the overall cholesterol absorption phenotype. By contrast, ACAT2$^{-/-}$ mice exhibited a slight upregulation of *Abcg5* mRNA expression (Fig. 2D), perhaps via an liver X receptor (LXR)-mediated response that might promote excretion of excess FC out of the cell and back into the lumen of the gut, which is also a factor that could potentially decrease cholesterol absorption.

In the absence of ACAT2, chylomicron assembly appeared to be intact, and *Mtp* and *ApoB* gene expression along the length of the SI were comparable across all genotypes (supplementary Table I). In agreement with previous reports (29, 41), *Abca1* mRNA expression appeared to be somewhat higher in ACAT2$^{-/-}$ mice compared with mice with intact ACAT2. However, this increase was modest and was only present in segments 1 and 2. Further, *Abca1* mRNA appeared to be higher in segments 2 and 3 of the ACAT2$^{+/-}$ mice, a response that was not observed in any other measurement in ACAT2$^{+/-}$ mice. However, the finding that <1% of radiolabeled sterols were detected in the plasma and in the liver after thoracic duct lymph collection suggests that efflux of unesterified cholesterol via ABCA1 on the basolateral side of the enterocyte was not a major factor determining cholesterol absorption efficiency. The mRNA levels of other cholesterol metabolism genes, such as *HmgCoAs, HmgCoAr,* and *Srebp-1c*, were very low and not different among genotypes. The low values

TABLE 1. Percentage composition of chylomicron particle mass

	% Particle Mass					
Genotype	Protein	PL	FC	TG	CE	Surface to Core
ACAT2$^{+/+}$	5.0 ± 0.7	11.7 ± 1.4	1.1 ± 0.2^a	69.9 ± 3.5^a	12.3 ± 1.9^a	0.2
ACAT2$^{+/-}$	4.1 ± 0.6	11.6 ± 0.9	1.2 ± 0.1^a	72.0 ± 3.5^a	11.1 ± 2.9^a	0.2
ACAT2$^{-/-}$	5.6 ± 1.2	10.8 ± 1.0	1.9 ± 0.1^b	80.6 ± 2.1^b	1.0 ± 0.4^b	0.2

Mass (µg) of protein, phospholipid (PL), free cholesterol (FC), triglyceride (TG), and cholesterol ester (CE) was measured in chylomicrons isolated from 8 hourly collections. The percent composition was calculated by dividing each component mass by the sum of all masses for each chylomicron sample from every time point. The mean percentage of all 8 time points from each animal was calculated for each particle component. The data expressed are the overall mean ± SEM for each genotype (n = 5/genotype). The surface-to-core ratio was calculated by dividing the sum of protein, PL, and FC by the sum of TG and CE. Different superscript letters denote statistically significant difference ($P < 0.05$) within the same column as measured by one-way ANOVA and Tukey posthoc tests.

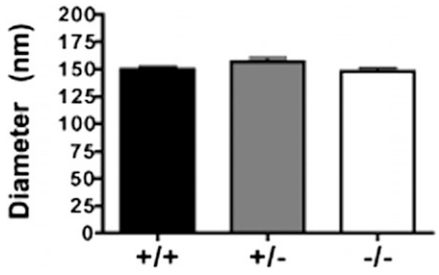

Fig. 7. Chylomicron particle size. Mean diameter of chylomicrons isolated from hour 3 and hour 4 lymph collections measured separately by dynamic light scattering (Zetasizer) and then averaged together. Data represent mean ± SEM (n = 5–8/genotype). No statistically significant difference ($P < 0.05$) was found by one-way ANOVA.

may indicate that an adaptation to the dietary cholesterol enrichment has taken place.

In this study, the TDLC technique yielded cholesterol absorption values that were comparable to values derived from the more commonly used FDI method, which indirectly estimates fractional cholesterol absorption by measuring radioactive sterol excretion into feces. The advantage of TLDC is that newly absorbed sterols in the lymph can be sampled over a time course and lipoproteins synthesized by the enterocyte (primarily chylomicrons) can be characterized in detail as in this study. This technique allows one to collect lymph from the thoracic lymph duct, which is the collecting point for all lymph vessels draining the GI tract, for a quantitative collection of intestinal lymph. Our experiments were conducted to carefully simulate physiologically relevant conditions. For example, to minimize the risk for postoperative ileus, we cannulated the duodenum with soft, flexible silicone tubing through the stomach and pyloric sphincter to minimize trauma to the intestine wall. We used a short-acting isoflurane for anesthesia and ketoprofen for analgesia, and the mice were allowed to move on an exercise wheel to coax lymph flow. A readily absorbable mixed micelle solution was used to deliver the bolus dose of radioactive sterols, and we used an intraduodenal constant infusion to help keep lymph

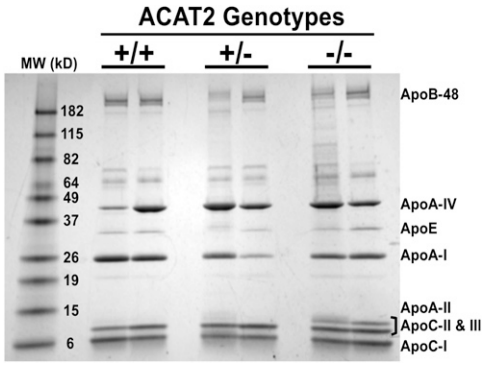

Fig. 8. Apolipoproteins of isolated chylomicron particles. Representative gel image of apolipoproteins on chylomicrons isolated from hour 3 lymph collection (n = 2/genotype). TCA-precipitated chylomicron proteins were separated on 4–20% SDS-PAGE gel and Coomassie stained for visualization.

flow constant. The intestine remained functional throughout the entire time course of the experiment, as evidenced by the fact that lymph flow rates did not decrease (supplementary Fig. II) and chylomicron secretion remained reasonably constant (Fig. 6). Finally, these studies were performed in the morning after mice had eaten a meal containing 20% of energy as fat and 0.2% cholesterol, a diet setting in which we have documented a role for ACAT2 in atherosclerosis (45).

At the end of the experiment, less than 1% of the total radioactive dose was found in the plasma and the liver of all mice, strongly indicating that significant amounts of newly absorbed cholesterol from the intestinal lumen did not directly enter the circulation via intestine-derived HDL particles as others have suggested (29, 40, 46). Instead, our data indicate that cholesterol absorption requires CE incorporation into chylomicron particles, which are then transported via the lymphatic system before entering the blood circulation at the subclavian vein. Brunham et al. (40) compared plasma HDL concentrations in intestinal-specific ABCA1 knockout mice to their wild-type counterparts and estimated that the intestine contributed ~30% of the plasma HDL pool. They also concluded that intestine-derived HDL particles are secreted directly into the circulation but not into the lymphatic system, because their mesenteric lymph duct cannulation experiments revealed almost undetectable amounts of [^{14}C]cholesterol in HDL-sized particles isolated from lymph. Our data would agree with the suggestion that newly absorbed cholesterol is not preferentially packaged into HDL particles for secretion into lymph. By contrast, our data argue that HDL synthesis by the enterocyte is not a significant pathway for dietary cholesterol absorption, as we found negligible amounts of radioactive cholesterol present in the plasma and the liver of our mice after 8 h of thoracic lymph duct cannulation.

We determined the characteristics of chylomicron particles by measuring particle size as well as by analyzing lipid and apolipoprotein compositions. Percentage distribution of [^{14}C]cholesterol and [^{3}H]sitosterol into free sterols versus sterol esters (Fig. 5) strongly supports the idea that ACAT2 preferentially esterifies cholesterol over phytosterols, which has been suggested by previous studies (43, 47). Although the average chylomicron particle sizes (~150 nm, Fig. 7) and the surface:core ratios (Table 1) were the same across all three genotypes, the chylomicron particle core was depleted of CE when ACAT2 was absent; by contrast, chylomicrons made by ACAT2$^{+/+}$ and ACAT2$^{+/-}$ mice contained both TG and CE. In the absence of ACAT2, most of the exogenous cholesterol molecules come into the body as FC that is primarily partitioned into the surface of the chylomicron particle among PL molecules and, apparently to a much lesser extent, dissolved in the TG-rich particle core. It was of interest that the apolipoprotein composition remained essentially unaffected in spite of this chemical difference in chylomicron composition (Fig. 8, Table 2).

Our findings show that, in ACAT2$^{-/-}$ mice, the percentage cholesterol absorption into lymph is consistently and significantly lower at all time points (Fig. 4), with chylomicron CE mass being virtually undetectable (Fig. 6E). Many

TABLE 2. Apolipoprotein profile of isolated chylomicron particles

	Percentage of Total Protein (n = 3/genotype)		
Apolipoproteins	ACAT2$^{+/+}$	ACAT2$^{+/-}$	ACAT2$^{-/-}$
B-48	10.7 ± 3.0	10.4 ± 2.3	11.7 ± 1.5
Unknown-1	2.5 ± 0.5	2.4 ± 0.2	1.7 ± 1.4
Unknown-2	6.6 ± 3.0	6.3 ± 3.8	5.6 ± 6.2
Albumin	4.8 ± 1.3	4.2 ± 0.4	5.3 ± 1.0
A-IV	17.0 ± 8.7	26.4 ± 4.1	15.7 ± 11.0
E	5.6 ± 0.8	3.1 ± 0.3	4.7 ± 2.8
A-I	18.8 ± 0.9	14.1 ± 4.5	14.5 ± 0.8
C-II, C-III, A-II	22.6 ± 3.8	23.3 ± 2.3	28.4 ± 7.8

TCA-precipitated chylomicron proteins were separated on 4–20% SDS-PAGE gel and Coomassie stained for visualization. Percentages of apolipoprotein composition were determined by densitometry (Alpha Innotech gel imager). Data shown are mean ± SD, n = 3/genotype.

have speculated that lack of CE formation would result in reduced cholesterol absorption, but we believe this study is the first to show that CE formation by ACAT2 selectively utilizes chylomicron particles for quantitative transport of newly absorbed cholesterol out of the enterocyte into the lymphatic system and subsequently into the body.

Altogether, these studies provide a strong line of evidence to support the hypothesis that the presence of ACAT2 maximizes cholesterol absorption efficiency by providing CE for incorporation into chylomicron particles. However, the data in the heterozygous ACAT2$^{+/-}$ mice indicate that ACAT2 wild-type mice have an excess of ACAT2 enzyme to accomplish the needed esterification, because ACAT2 wild-type and heterozygous mice both esterified and absorbed a similar amount of exogenous cholesterol. This outcome indicates that the prospect of reducing intestinal cholesterol absorption by inhibiting ACAT2 to reduce chylomicron-derived cholesterol from entering the circulation and ultimately preventing atherosclerosis does exist, but unfortunately, it will most likely require a rather complete inhibition of ACAT2 activity to result in an appreciable reduction of cholesterol absorption. Further studies are required to elucidate other molecular mechanisms or protein functions that may play critical roles in intestinal cholesterol absorption, perhaps by interacting with ACAT2.

The authors thank Dr. Martha D. Wilson and Mr. Ramesh Shah for their technical insights. We also wish to acknowledge the valuable guidance of Drs. Thomas L. Smith and Paolo Parini on our surgical approach, which was essential in moving this project forward.

REFERENCES

1. Rosamond, W., K. Flegal, K. Furie, A. Go, K. Greenlund, N. Haase, S. M. Hailpern, M. Ho, V. Howard, B. Kissela, et al. 2008. Heart disease and stroke statistics–2008 update: a report from the American Heart Association Statistics Committee and Stroke Statistics Subcommittee. *Circulation.* **117:** e25–e146.
2. Kannel, W. B., W. P. Castelli, T. Gordon, and P. M. McNamara. 1971. Serum cholesterol, lipoproteins, and the risk of coronary heart disease. The Framingham study. *Ann. Intern. Med.* **74:** 1–12.
3. Wang, D. Q. 2007. Regulation of intestinal cholesterol absorption. *Annu. Rev. Physiol.* **69:** 221–248.
4. McMurry, M. P., W. E. Connor, D. S. Lin, M. T. Cerqueira, and S. L. Connor. 1985. The absorption of cholesterol and the sterol balance in the Tarahumara Indians of Mexico fed cholesterol-free and high cholesterol diets. *Am. J. Clin. Nutr.* **41:** 1289–1298.
5. Iqbal, J., and M. M. Hussain. 2009. Intestinal lipid absorption. *Am. J. Physiol. Endocrinol. Metab.* **296:** E1183–E1194.
6. McGill, H. C. J. 1979. The relationship of dietary cholesterol to serum cholesterol concentration and to atherosclerosis in man. *Am. J. Clin. Nutr.* **32:** 2664–2702.
7. Dietschy, J. M., S. D. Turley, and D. K. Spady. 1993. Role of liver in the maintenance of cholesterol and low density lipoprotein homeostasis in different animal species, including humans. *J. Lipid Res.* **34:** 1637–1659.
8. Klein, R. L., and L. L. Rudel. 1983. Cholesterol absorption and transport in thoracic duct lymph lipoproteins of nonhuman primates. Effect of dietary cholesterol level. *J. Lipid Res.* **24:** 343–356.
9. Rudel, L. L., T. Mitamura, and J. M. Felts. 1973. Characterization of rabbit lymph chylomicra and very low density lipoproteins. *Circulation.* **252:** 47–48.
10. Hellman, L., E. L. Frazell, and R. S. Rosenfeld. 1960. Direct measurement of cholesterol absorption via the thoracic duct in man. *J. Clin. Invest.* **39:** 1288–1294.
11. Rudel, L. L., M. D. Morris, and J. M. Felts. 1972. The transport of exogenous cholesterol in the rabbit. I. Role of cholesterol ester of lymph chylomicra and lymph very low density lipoproteins in absorption. *J. Clin. Invest.* **51:** 2686–2692.
12. Hillyard, L. A., C. Entenman, I. L. Chaikoff, and W. O. Reinhardt. 1958. Composition and concentration of lymph and serum lipoproteins during fat and cholesterol absorption in the dog. *J. Biol. Chem.* **233:** 838–842.
13. Imaizumi, K., M. Fainaru, and R. J. Havel. 1978. Composition of proteins of mesenteric lymph chylomicrons in the rat and alterations produced upon exposure of chylomicrons to blood serum and serum proteins. *J. Lipid Res.* **19:** 712–722.
14. Chang, C. C., H. Y. Huh, K. M. Cadigan, and T. Y. Chang. 1993. Molecular cloning and functional expression of human acyl-coenzyme A:cholesterol acyltransferase cDNA in mutant Chinese hamster ovary cells. *J. Biol. Chem.* **268:** 20747–20755.
15. Cases, S., S. Novak, Y. W. Zheng, H. M. Myers, S. R. Lear, E. Sande, C. B. Welch, A. J. Lusis, T. A. Spencer, B. R. Krause, et al. 1998. ACAT-2, a second mammalian acyl-CoA:cholesterol acyltransferase. Its cloning, expression, and characterization. *J. Biol. Chem.* **273:** 26755–26764.
16. Lee, R. G., M. C. Willingham, M. A. Davis, K. A. Skinner, and L. L. Rudel. 2000. Differential expression of ACAT1 and ACAT2 among cells within liver, intestine, kidney, and adrenal of nonhuman primates. *J. Lipid Res.* **41:** 1991–2001.
17. Anderson, R. A., C. Joyce, M. Davis, J. W. Reagan, M. Clark, G. S. Shelness, and L. L. Rudel. 1998. Identification of a form of acyl-CoA:cholesterol acyltransferase specific to liver and intestine in nonhuman primates. *J. Biol. Chem.* **273:** 26747–26754.
18. Dreon, D. M., H. A. Fernstrom, H. Campos, P. Blanche, P. T. Williams, and R. M. Krauss. 1998. Change in dietary saturated fat intake is correlated with change in mass of large low-density-lipoprotein particles in men. *Am. J. Clin. Nutr.* **67:** 828–836.
19. Rudel, L. L., J. Haines, J. K. Sawyer, R. Shah, M. S. Wilson, and T. P. Carr. 1997. Hepatic origin of cholesteryl oleate in coronary artery atherosclerosis in African green monkeys. Enrichment by dietary monounsaturated fat. *J. Clin. Invest.* **100:** 74–83.
20. Rudel, L. L., J. S. Parks, L. Hedrick, M. Thomas, and K. Williford. 1998. Lipoprotein and cholesterol metabolism in diet-induced coronary artery atherosclerosis in primates. Role of cholesterol and fatty acids. *Prog. Lipid Res.* **37:** 353–370.
21. Klein, R. L., and L. L. Rudel. 1983. Effect of dietary cholesterol level on the composition of thoracic duct lymph lipoproteins isolated from nonhuman primates. *J. Lipid Res.* **24:** 357–367.
22. Dawson, P. A., and L. L. Rudel. 1999. Intestinal cholesterol absorption. *Curr. Opin. Lipidol.* **10:** 315–320.
23. Goodman, D. S. 1962. The metabolism of chylomicron cholesterol ester in the rat. *J. Clin. Invest.* **41:** 1886–1896.
24. Gage, S. H., and P. A. Fish. 1924. Fat digestion, absorption, and assimulation in man and animals as determined by the dark-field microscope, and a fat-soluble dye. *Am. J. Anat.* **34:** 1–85.
25. Buhman, K. K., M. Accad, S. Novak, R. S. Choi, J. S. Wong, R. L. Hamilton, S. Turley, and R. V. Farese, Jr. 2000. Resistance to diet-induced hypercholesterolemia and gallstone formation in ACAT2-deficient mice. *Nat. Med.* **6:** 1341–1347.
26. Rudel, L. L., K. Kelley, J. K. Sawyer, R. Shah, and M. D. Wilson. 1998. Dietary monounsaturated fatty acids promote aortic atherosclerosis

in LDL receptor null, human apoB100 overexpressing transgenic mice. *Arterioscler. Thromb. Vasc. Biol.* **18:** 1818–1827.
27. Kieft, K. A., T. M. A. Bocan, and B. R. Krause. 1991. Rapid on-line determination of cholesterol distribution among plasma lipoproteins after high-performance gel filtration chromatography. *J. Lipid Res.* **32:** 859–866.
28. Temel, R. E., L. Hou, L. L. Rudel, and G. S. Shelness. 2007. ACAT2 stimulates cholesteryl ester secretion in apoB-containing lipoproteins. *J. Lipid Res.* **48:** 1618–1627.
29. Temel, R. E., R. G. Lee, K. L. Kelley, M. A. Davis, R. Shah, J. K. Sawyer, M. D. Wilson, and L. L. Rudel. 2005. Intestinal cholesterol absorption is substantially reduced in mice deficient in both ABCA1 and ACAT2. *J. Lipid Res.* **46:** 2423–2431.
30. Wang, D. Q-H., and M. C. Carey. 2003. Measurement of intestinal cholesterol absorption by plasma and fecal dual-isotope ratio, mass balance, and lymph fistula methods in the mouse: an analysis of direct versus indirect methodologies. *J. Lipid Res.* **44:** 1042–1059.
31. Ionac, M. 2003. One technique, two approaches, and results: thoracic duct cannulation in small laboratory animals. *Microsurgery.* **23:** 239–245.
32. Lowry, O. H., N. J. Rosebrough, A. L. Farr, and R. J. Randall. 1951. Protein measurement with the Folin phenol reagent. *J. Biol. Chem.* **193:** 265–275.
33. Iverson, S. J., S. L. Lang, and M. H. Cooper. 2001. Comparison of the Bligh and Dyer and Folch methods for total lipid determination in a broad range of marine tissue. *Lipids.* **36:** 1283–1287.
34. Fiske, C. H., and Y. Subbarow. 1925. The colorimetric determination of phosphorus. *J. Biol. Chem.* **66:** 375–400.
35. Fidge, N. H., and P. J. McCullagh. 1981. Studies on the apoproteins of rat lymph chylomicrons: characterization and metabolism of a new chylomicron-associated apoprotein. *J. Lipid Res.* **22:** 138–146.
36. Lee, R. G., R. Shah, J. K. Sawyer, R. L. Hamilton, J. S. Parks, and L. L. Rudel. 2005. ACAT2 contributes cholesteryl esters to newly secreted VLDL, whereas LCAT adds cholesteryl ester to LDL in mice. *J. Lipid Res.* **46:** 1205–1212.
37. Lee, R. G., K. L. Kelley, J. K. Sawyer, R. V. Farese, Jr., J. S. Parks, and L. L. Rudel. 2004. Plasma cholesterol esters provided by lecithin:cholesterol acyltransferase and acyl-coenzyme A:cholesterol acyltransferase 2 have opposite atherosclerotic potential. *Circ. Res.* **95:** 998–1004.
38. Alger, H. M., J. M. Brown, J. K. Sawyer, K. L. Kelley, R. Shah, M. D. Wilson, M. C. Willingham, and L. L. Rudel. 2010. Inhibition of acyl-coenzyme A:cholesterol acyltransferase 2 (ACAT2) prevents dietary cholesterol-associated steatosis by enhancing hepatic triglyceride mobilization. *J. Biol. Chem.* **285:** 14267–14274.
39. Repa, J. J., K. K. Buhman, R. B. Farese, Jr., J. M. Dietschy, and S. D. Turley. 2004. ACAT2 deficiency limits cholesterol absorption in the cholesterol-fed mouse: impact on hepatic cholesteol homeostasis. *Hepatology.* **40:** 1088–1097.
40. Brunham, L. R., J. K. Kruit, J. Iqbal, C. Fievet, J. M. Timmins, T. D. Pape, B. A. Coburn, N. Bissada, B. Staels, A. K. Groen, et al. 2006. Intestinal ABCA1 directly contributes to HDL biogenesis in vivo. *J. Clin. Invest.* **116:** 1052–1062.
41. Turley, S. D., M. A. Valasek, J. J. Repa, and J. M. Dietschy. 2010. Multiple mechanisms limit the accumulation of unesterified cholesterol in the small intestine of mice deficient in both ACAT2 and ABCA1. *Am. J. Physiol. Gastrointest. Liver Physiol.* **299:** G1012–G1022.
42. Turkish, A. R., A. L. Henneberry, D. Cromley, M. Padamsee, P. Oelkers, H. Bazzi, A. M. Christiano, J. T. Billheimer, and S. L. Sturley. 2005. Identification of two novel human acyl-CoA wax alcohol acyltransferases: members of the diacylglycerol acyltransferase 2 (DGAT2) gene superfamily. *J. Biol. Chem.* **280:** 14755–14764.
43. Temel, R. E., A. K. Gebre, J. S. Parks, and L. L. Rudel. 2003. Compared with acyl-CoA:cholesterol O-acyltransferase (ACAT)1 and lecithin:cholesterol acyltransferase, ACAT2 displays the greatest capacity to differentiate cholesterol from sitosterol. *J. Biol. Chem.* **278:** 47594–47601.
44. Davis, H. R., Jr., L. J. Zhu, L. M. Hoos, G. Tetzloff, M. Maguire, J. Liu, X. Yao, S. P. Iyer, M. H. Lam, E. G. Lund, et al. 2004. Niemann-Pick C1 Like 1 (NPC1L1) is the intestinal phytosterol and cholesterol transporter and a key modulator of whole-body cholesterol homeostasis. *J. Biol. Chem.* **279:** 33586–33592.
45. Bell 3rd, T. A., J. M. Brown, M. J. Graham, K. M. Lemonidis, R. M. Crooke, and L. L. Rudel. 2006. Liver-specific inhibition of acyl-coenzyme a:cholesterol acyltransferase 2 with antisense oligonucleotides limits atherosclerosis development in apolipoprotein B100-only low-density lipoprotein receptor−/− mice. *Arterioscler. Thromb. Vasc. Biol.* **26:** 1814–1820.
46. Field, F. J., K. Watt, and S. N. Mathur. 2008. Origins of intestinal ABCA1-mediated HDL-cholesterol. *J. Lipid Res.* **49:** 2605–2619.
47. Field, F. J., and S. N. Mathur. 1983. beta-sitosterol: esterification by intestinal acylcoenzyme A:cholesterol acyltransferase (ACAT) and its effect on cholesterol esterification. *J. Lipid Res.* **24:** 409–417.